Available online at www.sciencedirect.com

SciVerse ScienceDirect

Ceramics International 38 (2012) 6769–6775

CERAMICS INTERNATIONAL

www.elsevier.com/locate/ceramint

Hercynite and magnesium aluminate spinels acting as a ceramic bonding in an electrofused MgO–$CaZrO_3$ refractory brick for the cement industry

Edén Rodríguez[a,*], G-Alan Castillo[a], José Contreras[a], R. Puente-Ornelas[a], J.A. Aguilar-Martínez[b], Laura García[a], Cristian Gómez[a]

[a] *Universidad Autónoma de Nuevo León (UANL), Facultad de Ingeniería Mecánica y Eléctrica (FIME), Programa Doctoral en Ingeniería de Materiales; Nuevo León, México 066451, Mexico*

[b] *Centro de Investigación en Materiales Avanzados, S.C. (CIMAV); Alianza Norte No. 202, Parque de Investigación e Innovación Tecnológica (PIIT), Nueva carr. Aeropuerto Km. 10 Apodaca N.L. México 66600, Mexico*

Received 5 April 2012; received in revised form 20 May 2012; accepted 22 May 2012
Available online 30 May 2012

Abstract

Innovative chrome-free basic refractory bricks have been design based on electrofused magnesia–calcium zirconate (MgO-$CaZrO_3$) technology using as ceramic bonding magnesium aluminate spinel ($MgAl_2O_4$) and hercynite spinel ($FeAl_2O_4$) in order to improve their properties. Industrial refractory bricks have been manufactured by solid state sintering of magnesium and calcium zirconate aggregates with $MgAl_2O_4$ and $FeAl_2O_4$ spinels at 1650 °C in a tunnel kiln. Physical and microstructural characteristics of new refractory bricks have been characterised in terms of density, porosity, crystalline phases, phase distribution and morphology. X-ray diffraction (XRD) analyses and scanning electron microscopy (SEM) with microanalysis (using energy dispersive spectroscopy analysis -EDS) have been used. The mechanical behaviour has been evaluated in terms of cold crushing strength (CCS) at room temperature and three point bending modulus of rupture (MOR) at 25 and 1260 °C. Static and dynamic resistance test by chemical attack of clinker raw meal constituents have been carried out at 1450 °C. Results have shown that thermo-mechanical properties of new refractory bricks significantly improved with increasing both type of spinel in content. Microstructural analysis revealed that spinel phases aided to develop a strong bond between the magnesia and calcium zirconate refractory aggregates. Finally, these refractory matrixes exhibit a good thermal stability and an excellent chemical resistance against clinker raw meal.

Keywords: E. MgO–$CaZrO_3$ refractories; D. Hercynite; B. Ceramic bonding; E. Rotary cement kiln

1. Introduction

Recently, the substitution of fossil fuels by the use of secondary fuels and industrial waste (e.g. used tires, coal ash and sewage sludges), associated with the modernisation and improvements of the cement rotary kiln themselves have drastically affected the performance life of the refractory bricks [1–6]. Those changes have driven the refractory industry to create and develop improved refractory lining products.

Newest refractory trends, for improving the properties of lining are related to the optimisation of the matrix by careful design of phase combinations and the microstructure characteristics. There is no doubt that, one of the main microstructural characteristic that has to taking into account for contributing to the development of a reliable refractory matrix is the bond. By increasing the bonding strength, the resistance against many kinds of stresses during performance and structural spalling would be improved. In addition, a high strength brick frequently has been linked to a rigid matrix; however cement rotary

*Corresponding author. Tel.: +52 81 83294020x1619; fax: +52 81 83294020.
E-mail addresses: earc22@hotmail.com, eden_amaral_rdz_c@hotmail.com (E. Rodríguez).

0272-8842/$36.00
http://dx.doi.org/10.1016/j.ceramint.2012.05.071

kilns require refractory bricks with sufficient structural flexibility and stress absorbent to prevent cracking and peeling off from the hot face.

By other hand, MgO–$CaZrO_3$ materials are well known to be compatible phases, do not form a liquid phase up to temperatures higher than 2060 °C and they are highly resistant in aggressive basic environments and atmospheres with high alkali contents at temperature up to 1400 °C. In this kind of refractory matrix, the formation of a so-called elastic direct bonding between MgO and $CaZrO_3$ and the high refractoriness of $CaZrO_3$ (2340 °C), allow to reach a high hot mechanical strength and excellent corrosion resistance against alkali, earth alkali oxides and basic slags [7–20]. Kozuka et al. [21,22] in Japan have studied the behaviour of magnesia–calcium zirconate refractory bricks in rotary cement kilns. The conclusion of this study proved that the bricks showed superior corrosion resistance and good coating adherence but peeled off easily in high stressed areas.

The Phase equilibria in the system CaO–MgO–Al_2O_3–ZrO_2 and the binary subsystems $CaAl_2O_4$–$CaZrO_3$ and $MgAl_2O_4$–$CaZrO_3$ and the isothermal sections at 1650 °C of the systems $MgAl_2O_4$–$CaAl_2O_4$–$CaZrO_3$ and MgO–$CaAl_2O_4$–$CaZrO_3$ have been investigated by Liddle and Brett [23]. One of their conclusions was that the liquid phase between $MgAl_2O_4$ and $CaZrO_3$ can appear at the temperature above 1650 °C by mass proportion 40:60 ($MgAl_2O_4$:$CaZrO_3$).

According to the above mentioned, the objectives of this research are the study, development and the evaluation of physical, mechanical, thermo-mechanical and chemical properties, as well as microstructural characteristics of a new free-chrome refractory brick composes of a matrix made of electrofused magnesia–calcium zirconate (MgO–$CaZrO_3$) with small addition of magnesium aluminate spinel ($MgAl_2O_4$) and hercynite ($FeAl_2O_4$) acting as ceramic bonding. Therefore, due to the importance of developing a strong bonding structure in the refractory matrixes, the influence of varying the amount of both spinel phases ($MgAl_2O_4$ and $FeAl_2O_4$) on the refractory matrix was established in this investigation. Additionally, static and dynamic resistance tests to chemical attack by clinker raw meal were carried out.

2. Experimental procedure

2.1. Raw material

Since, raw material characteristics play an important role in getting suitable final refractory properties; the use of high purity raw material was a necessary matter (even in industrial scale). The chemical composition of the raw material used for the development of new refractory bricks is given in Table 1. For the sintered magnesia a wide particle size distribution (coarse, intermediate and fine grains) was used; for electrofused magnesia–calcium zirconate mixture, only coarse and intermediate grains were used. Fine particle grains (less than 45 μm) were utilised for ZrO_2, $MgAl_2O_4$ and $FeAl_2O_4$. The addition of a fine particle size for spinel and zirconia is due to a well known superior reaction force with the surrounding matrix (in Table 2 is given the particle size distribution of raw meals). The crystalline phases identified by XRD analysis for the starting raw meal were: MgO (periclase-MgO), MgO–$CaZrO_3$ (periclase-MgO, calcium zirconate-$CaZrO_3$),

Table 1
Chemical composition of raw materials.

	Compositions (% by weight)					
Raw material	MgO	ZrO_2	CaO	Al_2O_3	Fe_2O_3	SiO_2
Sintered MgO	98.91	–	0.85	0.08	0.05	0.11
Elecrofused MgO–$CaZrO_3$	50.00	36.43	13.57	–	–	–
$MgAl_2O_4$	34.00	–	0.20	64.0	1.0	0.40
$FeAl_2O_4$	4.6	–	0.19	49.06	45.78	0.13
ZrO_2	–	97.72	–	–	–	2.10

Table 2
Particle size distribution of raw materials.

	Particle size distribution			
Mesh number (Tyler)	**MgO**	**$CaZrO_3$**	**$MgAl_2O_4$ $FeAl_2O_4$**	**ZrO_2**
−4+7	7.0	20.0	–	–
−7+14	29.0	44.0	–	–
−14+28	22.0	28.0	–	–
−28+60	12.0	8.0	–	–
−60	6.0	–	–	–
−325	24.0	–	100	100

$MgAl_2O_4$ (periclase-MgO and spinel-$MgAl_2O_4$), $FeAl_2O_4$ (hercynite-$FeAl_2O_4$) and ZrO_2 (baddeleyite-ZrO_2).

2.2. Refractory matrix

In order to evaluate the effect of magnesium aluminate and hercynite spinels on an electrofused MgO–$CaZrO_3$ matrix, nine refractory formulations were studied; the first one without addition of spinel (MZ brick) and the rest with variations in the spinel content. Refractory formulations are shown in Table 3. The addition of a small amount of fine zirconia particles in all formulations responds mainly to avoid free lime in the refractory matrix through a possible formation of an *in situ* calcium zirconate phase.

2.3. Preparation and characterisation of refractory bricks

Mixtures with compositions according to proportions given in Table 3 were prepared. Dextrine was added to bind mixtures and for providing maximum stability to the green ceramic compacts during subsequent handling prior to firing. Powders were uniaxial pressed into a metallic mould obtaining refractory bricks of $228 \times 114 \times 76$ mm. After pressing, green bricks were sintering at 1650 °C for 7 h in an industrial tunnel kiln. Physical properties such as apparent porosity, bulk density, cold crushing strength, cold modulus of rupture and hot modulus of rupture at 1260° C were measured based on ASTM standards. Phase analyses of the sintered brick were carried out by X-ray diffraction study (Philips X′pert) using equipment using, CuK_α radiation source ($\lambda = 1.54056$ Å) and a setting of 40 Kv and 30 mA. All XRD data were collected under the same experimental conditions; in the angular range $10^\circ \leq 2\theta \leq 70^\circ$ using $\theta/2\theta$ configuration with a step scan of 0.05° 2θ and 1 s per step exposure time. Sintered bricks morphology was examined using scanning electron microscope (JSM-6490, Joel) with an energy dispersive spectrometer (EDS) attachment for qualitative and quantitative microanalysis.

Static and dynamic chemical attack test by clinker raw meal powders (see Table 4) were executed for evaluating corrosion resistence and coatability of free-spinel MgO–$CaZrO_3$ matrix and MgO–$CaZrO_3$ matrixes with spinel addition. The static method intends to make raw meal contact with the refractory and evaluates clinker adherences by heating. Using a crucible ($114 \times 114 \times 76$ mm) made of refractory brick, a hole was bored in the sample brick with the dimensions $\Phi 50 \times 50$ mm and filled it with clinker raw meal. The crucible sample was heated in a gas furnace for 4 h at 1450 °C. The adherence of the clinker on the refractory was determined according to the following criteria: nill adherence (clinker pellet is removed by inverting the sample up side down), moderate adherence (clinker pellet is removed by slightly hitting) and strong adherence (clinker pellet is practically fused with the refractory).

For the dynamic method a laboratory rotary kiln was lined with the refractory to be tested. The temperature was increased to 145 °C with an air/O_2 burner. The raw meal (the amount of 3–5 kg) was fed continually during 4 h rotating the kiln at 1 r.p.m. After the test, the degree of penetration and the microstructure damage of the refractory were evaluated by electronic microscopy on polished sections.

Table 3
Refractory formulations.

	Compositions (% by weight)				
Brick type	**MgO**	**$CaZrO_3$**	**$MgAl_2O_4$**	**$FeAl_2O_4$**	**ZrO_2**
MZ	85.5	14.0	–	–	0.5
2S	83.0	14.0	2.5	–	0.5
3S	81.9	14.0	3.6	–	0.5
4S	80.7	14.0	4.8	–	0.5
5S	79.5	14.0	6.0	–	0.5
6H	83.0	14.0	–	2.5	0.5
7H	81.9	14.0	–	3.6	0.5
8H	80.7	14.0	–	4.8	0.5
9H	79.5	14.0	–	6.0	0.5

Table 4
Chemical composition of clinker raw meal.

Compositions (% by weight)						
CaO	SiO_2	Al_2O_3	Fe_2O_3	MgO	K_2O	Na_2O
44.79	11.86	3.03	1.60	0.88	0.47	0.24

3. Results and discussion

3.1. Physical properties

Physical properties of each type of studied bricks in this investigation are provided in Table 5. According to results an average magnitude of apparent porosity for refractory bricks was established around 17–18%. Whereas the porosity of refractory bricks manifests itself in different coating adhesion levels, the average magnitude reached in this study was suitable because it could permit a desirable good coating adherence avoiding thermal overloads on the brick hot face.

Results obtained for cold crushing strength shown an increase tendency in magnitude with spinel addition and a maximum cold crushing strength magnitude corresponding to 3S brick for magnesium aluminate spinel ($MgAl_2O_4$) and 9H refractory brick for hercynite spinel ($FeAl_2O_4$). This behaviour can be explained in porosity terms, since according to those values 3S and 9H refractory bricks registered the minimum porosity magnitude. Taking into account the cold crushing strength value registered by MZ brick, there was a maximum increase in resistance of 42.67% and 40.15% with the addition of $MgAl_2O_4$ and $FeAl_2O_4$ spinels, respectively.

For cold and hot modules of rupture the addition of both magnesium aluminate and hercynite spinels resulted

Table 5
Physical properties of the refractory bricks.

Brick type	Properties				
	Apparent porosity (%)	Bulk density (g/cm^3)	Cold crushing strength (MPa)	Modulus of rupture (MPa)	Hot modulus of rupture at 1260 °C (Mpa)
MZ	18.4	2.94	39.6	9.6	5.7
2S	17.7	3.01	54.2	12.7	14.1
3S	17.1	3.02	56.5	11.6	12.3
4S	18.1	2.98	47.2	8.7	11.3
5S	18.6	2.97	49.3	9.5	11.8
6H	18.4	3.00	44.2	9.7	10.8
7H	18.2	3.01	49.4	10.5	11.5
8H	18.1	3.00	47.5	10.4	12.9
9H	17.9	3.00	55.5	11.2	7.84

in higher magnitudes compared to MZ brick. In addition, it was found that the most favourable spinel content to reaches the maximum value in both cold and hot modules of rupture was that amount contains in the 2S refractory brick for $MgAl_2O_4$ and the addition contains in 8H refractory brick for $FeAl_2O_4$. The improvement in cold modulus of rupture by the addition of $MgAl_2O_4$ and $FeAl_2O_4$ spinels was 32.9% and 5.2%, respectively. Finally, there was a maximum increment in hot modulus of rupture of 144% and 123% for $MgAl_2O_4$ and $FeAl_2O_4$ spinels addition, respectively

3.2. X-ray diffraction analysis

The X-ray diffraction (XRD) study obtained from each refractory brick revealed the presence of the same phases prior to sintering. The phase analysis in the refractory matrix without spinel addition (neither $MgAl_2O_4$ nor $FeAl_2O_4$) showed periclase (MgO), as well as calcium zirconate ($CaZrO_3$). This indicates that there is no sign of new phases formed.

Small peaks related to the magnesium aluminate spinel could be identified in XRD patterns of bricks with different spinel contents (2S–5S) at $2\theta = 43$, 53 and 18. The intensity of $MgAl_2O_4$ peaks almost does not increase at higher spinel addition (Fig. 1). XRD patterns of bricks with different hercynite contents (6H–9H) indicate the presence of MgO and $CaZrO_3$ as well as very small peaks related to hercynite spinel identified in XRD patterns at $2\theta = 34$ and 44. The intensity of $FeAl_2O_4$ peaks almost is the same at higher spinel addition (Fig. 2).

3.3. Microstructural analysis

Fig. 3 shows a SEM image of the sintered microstructure of the brick without spinel content (MZ brick). It can be observed a homogeneous microstructure matrix forms by two well-distributed phases. Using energy dispersive spectroscopy analysis (EDS) were identified as magnesia (dark grey grains) and calcium zirconate (light grey grains).This microstructure showed calcium zirconate aggregates (fused

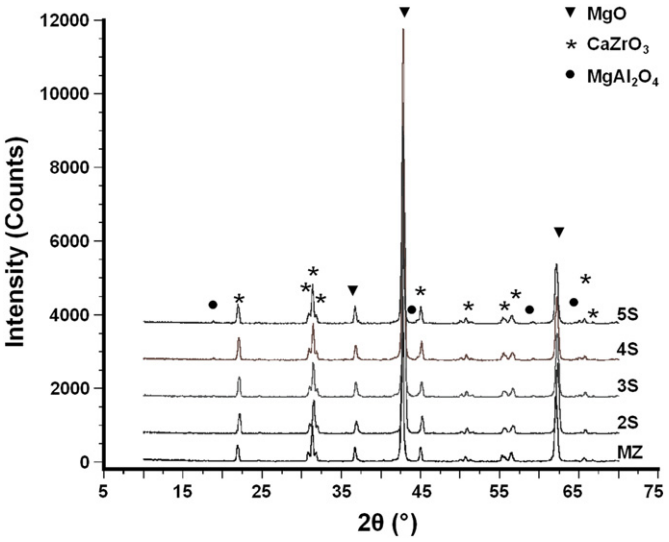

Fig. 1. Comparative XRD phase analysis between MZ refractory brick and bricks with $MgAl_2O_4$ spinel addition (2S, 3S, 4S and 5S).

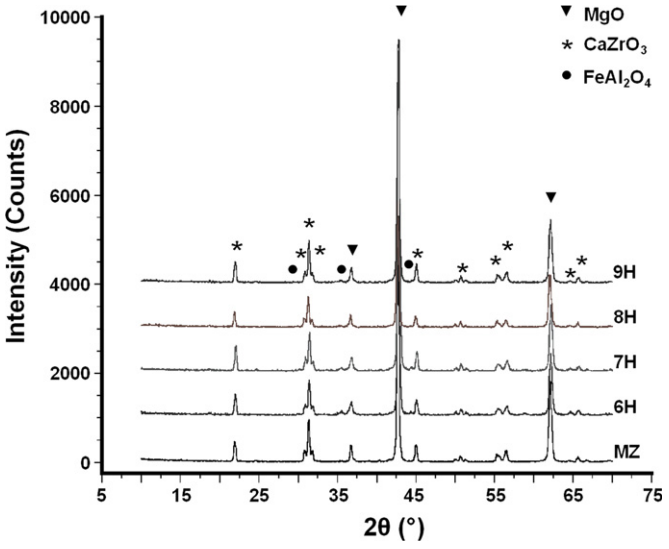

Fig. 2. Comparative XRD phase analysis between MZ refractory brick and bricks with $FeAl_2O_4$ spinel addition (6H, 7H, 8H and 9H).

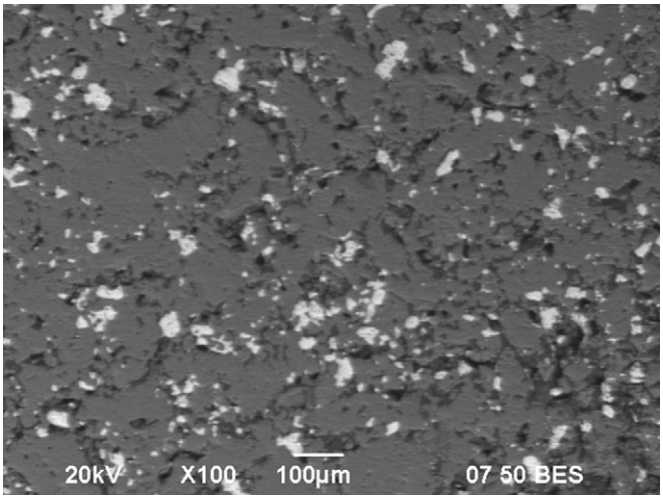

Fig. 3. MZ brick (see Table 3). Calcium zirconate (light grey grains) aggregates surrounded by the periclase (dark grey grains) groundmass.

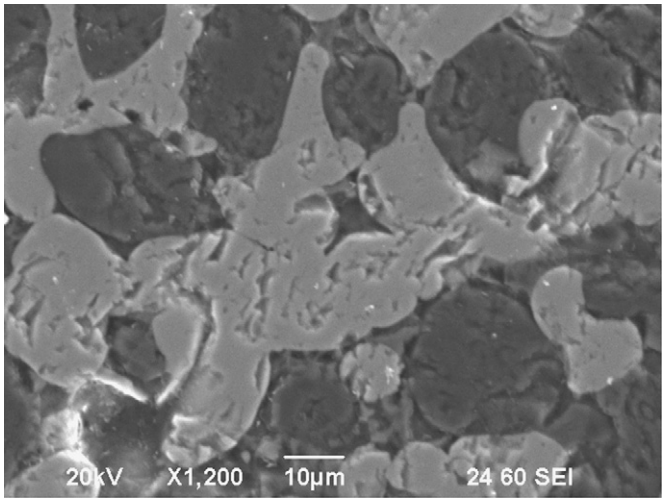

Fig. 4. General microstructure of refractory bricks with $MgAl_2O_4$ spinel addition. There are well-distributed magnesia (dark grey grains) and calcium zirconate grains (light grey grains) in the microstructure as mainly phases.

grains) surrounded by the periclase groundmass. At higher magnification an excellent bond linkage between MgO and $CaZrO_3$ grains was observed.

In the Fig. 4, it was shown a representative microstructure corresponding to refractory bricks with addition of $MgAl_2O_4$ spinel (2S, 3S, 4S and 5S). This microstructural analysis revealed as in MZ brick, the presence of well-distributed magnesia (dark grey grains) and calcium zirconate grains (light grey grains) in the microstructure as mainly phases. In this microstructure also calcium zirconate aggregates (fused grains) are surrounded by the periclase groundmass. Magnesium aluminate spinel phase was not identified at low magnifications; however, at higher magnifications it was revealed that spinel was located in the boundaries between MgO and $CaZrO_3$ particles possibly acting as a ceramic bonding among two these phases (the presence of spinel was corroborated through several microstructural analyses by EDS technique at high magnification).

It is proposed that spinel ($MgAl_2O_4$) phase was localised by diffusion in these specific zones due to its melting temperature is lower than both magnesia and calcium zirconate phases. Besides, the fine particle size of spinel phase contributed to the arrangement in those specific zones. A high magnification SEM image for 5S brick is shown in Fig. 5, in which spinel phase was identified in the boundaries between magnesia and calcium zirconate particles. The detailed EDS analysis on this surface (labelled $MgAl_2O_4$ in Fig. 5) revealed the presence of Mg and Al on the boundary between MgO and $CaZrO_3$.

The representative microstructure corresponding to the refractory formulations with addition of $FeAl_2O_4$ spinel (6H, 7H, 8H and 9H) is shown in Fig. 6. By this analysis, it can be seen in the microstructure the presence of well-distributed magnesia (dark grey grains) and calcium zirconate grains (light grey grains) as mainly phases. Through several analyses at high magnifications, hercynite spinel was also located in the boundaries between MgO and $CaZrO_3$ particles possibly acting as a ceramic bonding between these phases. This was corroborated by EDS analysis. $FeAl_2O_4$ spinel could be localised by diffusion in these zones due to its lower melting point compared to MgO and $CaZrO_3$ phases.

Small particles of spinel ($MgAl_2O_4$, $FeAl_2O_4$) located at the grain boundaries and triple points of the coarse aggregate of electrofused MgO–$CaZrO_3$, are not compatible with the $CaZrO_3$ and MgO. Because of this, the sintering process of these materials takes place in the presence of liquid phase (the liquid phase in the current system, represented by $MgAl_2O_4$ and $FeAl_2O_4$ spinels could be acting as a ceramic bonding). As it was predicted by Liddle and Brett [23], the liquid phase could appear

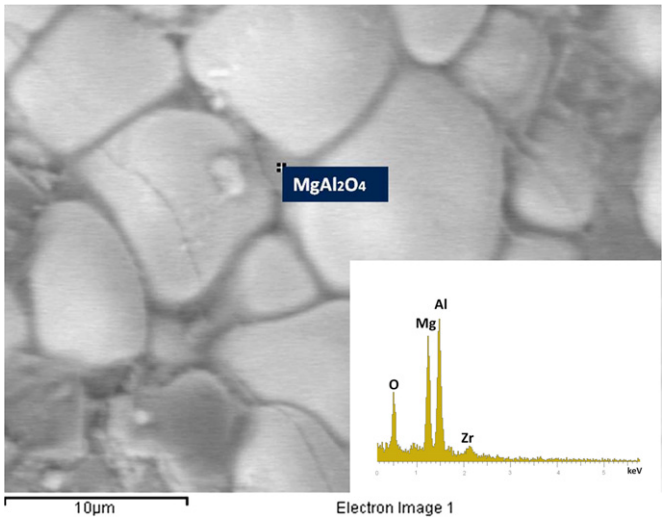

Fig. 5. SEM micrograph of the 5S refractory brick. SEM Image and EDS analysis suggesting the presence of $MgAl_2O_4$, the rectangle area indicates the spinel location in the microstructure.

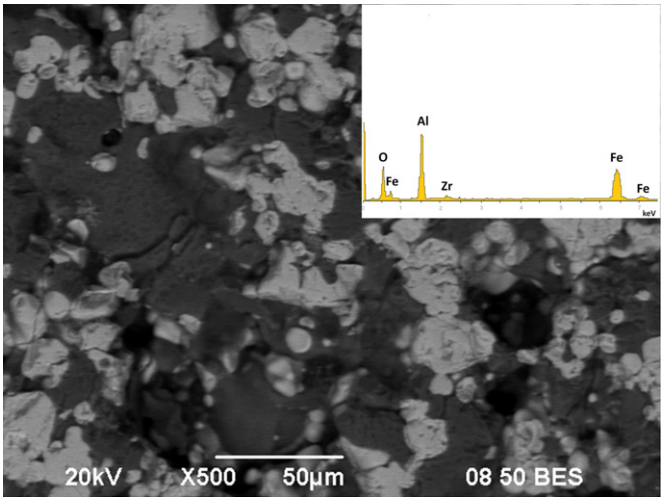

Fig. 6. General microstructure of refractory bricks with $FeAl_2O_4$ spinel addition. Calcium zirconate (light grey grains) aggregates surrounded by a periclase groundmass (dark grey grains) and pores (black spot). EDS analysis suggesting the presence of $FeAl_2O_4$, between MgO and $CaZrO_3$ grains.

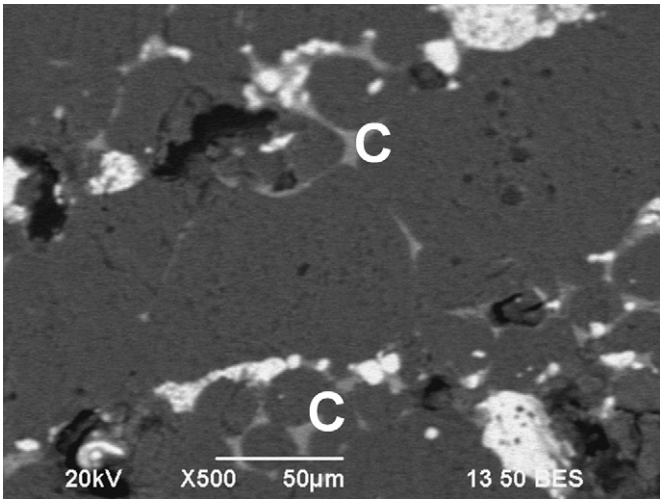

Fig. 7. General microstructure of refractory bricks with $MgAl_2O_4$ spinel addition tested with clinker raw meal at 1450 °C for 4 h. Clinker phases (C) as interstitial substances between periclase grains (dark grey) and calcium zirconate grains (light grey).

Table 6
Adherence test with clinker raw meal.

Brick type	Static test		Dynamic test
	Distance from hot face (mm)	Adherence	Adherence
MZ	9.0	Strong	Moderate
2S	6.4	Strong	Moderate
3S	5.6	Strong	Moderate
4S	5.7	Moderate	Moderate
5S	5.7	Moderate	Moderate
6H	3.6	Moderate	Moderate
7H	3.4	Moderate	Moderate
8H	4.3	Nil	Moderate
9H	5.5	Nil	Moderate

between $MgAl_2O_4$ and $CaZrO_3$ at above 1650 °C. The appearance of the liquid phase below this temperature is related to the presence of transition phases as the calcium aluminates. For $CaO–MgO–Al_2O_3$ system, in $MgO–C_{12}A_7–C_3A$ co-stability triangle, the liquid phase appeared at 1321 °C as the eutectic point [24].

3.4. Coatability and corrosion resistance

In Table 6 is shown the results obtained by static and dynamic methods for determining the coating adhesion in the refractory bricks. In general through a visual inspection, the hot face in every refractory was no corroded by clinker liquid phases; however a brown molten phase entered up to a range of 6–9 mm depth. According to this test, the MZ refractory brick showed the maximum coating adherence having a good correlation taking into account the porosity percentage since MZ brick reached the maximum porosity value. Besides, $CaZrO_3$ is very compatible with clinker phases, permitting a good coating adherence. For refractory bricks doped with spinel ($MgAl_2O_4$), there is a strong tendency to coating adherence at low spinel contents; however at higher contents the coating adherence becomes moderate in spite of a porosity value similar to that registered by MZ brick. This behaviour could be explain since spinel ($MgAl_2O_4$) has a well known lack of coating adherence and therefore does not contribute to coating adherence. Results of refractory bricks doped with hercynite spinel ($FeAl_2O_4$) showed a clear tendency to diminish the coating adherence while spinel contents get increase.

The examination of penetrated region by cement clinker in accordance to the microstructural analysis corresponding to static and dynamic tests resulted in a slightly densification without corrosion evidence; i.e. areas close to clinker did not suffer any kind of alteration taking into account the phase colours. It is important to mention that bonding strength still remained in all refractory bricks. Figs. 7 and 8 revealed a slightly dense microstructure showed in all bricks due to the penetration of clinker phases. These clinker phases (labelled as C in Fig.7 and 8) are located as interstitial substances between periclase grains (dark grey) and calcium zirconate grains (light grey). Besides, a magnesia–calcium zirconate unaltered bonding was observed.

4. Conclusions

Our research demonstrated that the addition of magnesium aluminate and hercynite spinels to the electrofused $MgO–CaZrO_3$ brick improved their thermo-mechanical properties. The microstructural analysis revealed that both spinel ($MgAl_2O_4$ and $FeAl_2O_4$) were located in boundaries

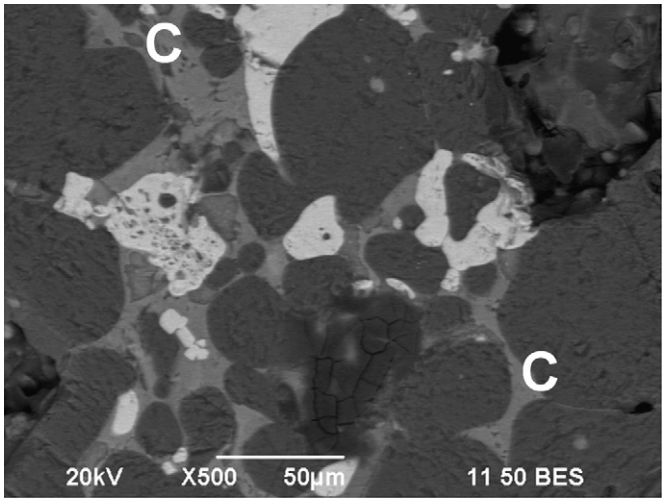

Fig. 8. General microstructure of refractory bricks with $FeAl_2O_4$ spinel addition tested with clinker raw meal at 1450 °C for 4 h. Clinker phases (C) as interstitial substances between periclase grains (dark grey) and calcium zirconate grains (light grey).

between MgO and $CaZrO_3$ particles acting as a bond linkage among these phases. Small particles of spinel ($MgAl_2O_4$, $FeAl_2O_4$), located at the grain boundaries and triple points of the coarse aggregate of electrofused MgO–$CaZrO_3$, are not compatible with the $CaZrO_3$ and MgO. Because of this, the sintering process of these materials takes place in the presence of liquid phase (the liquid phase in the current system, represented by $MgAl_2O_4$ and $FeAl_2O_4$ spinels could be acting as a ceramic bonding). Coating adherence was moderate and a general slightly dense microstructure with a magnesia–calcium zirconate unaltered bonding was presented after raw meal clinker attack.

References

[1] P. Bartha, H.J. Klischat, Classification of magnesia bricks in rotary cement kilns according to specification and service-ability, ZKG International 47 (1994) 277–280.
[2] J. Szczerba, The mechanisms of new phases formation in basic refractories in reaction with sintering cement clinker, Ceramika/Ceramics 102 (2008) 151–170.
[3] H.J. Klischat, P. Bartha, Progress in performance behavior of basic bricks by innovative raw material selection, in: Proceedings of the 7th UNITECR' 01, 2001, pp. 631–641.
[4] J. Szczerba, Examples of changes in magnesia spinel bricks after working in cement dry-process kilns using alternative fuels, in: Proceedings of the 1st Global Refractories for Cement and Lime Conference and Exhibition, London, 2007, pp. 4.1–4.8.
[5] R.H. Bogue, The Chemistry of Portland Cement, Reinhold Publishing Corporation, New York, 1955, pp. 355–364.
[6] J. Szczerba, Changes in basic brick from preheater cement kilns using secondary fuels, Industrial Ceramics 29 (2009) 19–30.
[7] J.L. Rodríguez-Galicia, A.H. de Aza, J.C. Rendón-Angeles, P. Pena, The mechanism of corrosion of MgO $CaZrO_3$–calcium silicate materials by cement clinker, Journal of European Ceramic Society 27 (2007) 79–89.
[8] S. Serena, MA. Sainz, A. Caballero, Corrosion behavior of MgO/$CaZrO_3$ refractory matrix by clinker, Journal European Ceramic Society 24 (2004) 2399–2406.
[9] S. Serena, M.A. Sainz, A. Caballero, The system clinker– MgO–$CaZrO_3$ and its application to the corrosion behavior of $CaZrO_3$/MgO refractory matrix by clinker, Journal European Ceramic Society 29 (2009) 2199–2209.
[10] Edén Rodríguez, G-Alan Castillo, José Contreras, J.A. Aguilar Martínez, Yadira González, Ana-María Guzmán, Laura I. García Ortiz, Desarrollo de un refractario MgO-CaZrO3 dopado con MgAl2O4 para la industria cementera, Ciencias UANL 15 (2011) 23–30.
[11] Edén Rodríguez, G-Alan Castillo, Ana María Guzmán, Effect of spinel $MgAl_2O_4$ on microstructural and mechanochemical properties evolution in a sintered MgO–$CaZrO_3$ refractory matrix, Industrial Ceramics 31 (2011) 1–5.
[12] E.A. Rodríguez, G.A. Castillo and A.M. Guzmán, Development of a chrome-free refractory based on electrofused magnesia–calcium zirconate technology using spinel addition for use in cement rotary kilns, in: Proceedings of the 11th UNITECR' 09, 2009, pp. 72.
[13] J.L. Rodríguez, C. Baudín, P. Pena, Relationships between phase constitution and mechanical behaviour in MgO–$CaZrO_3$–calcium silicate materials, Journal of European Ceramic Society 24 (2004) 669–679.
[14] J.L. Rodríguez, P. Pena, Obtención de materiales de magnesia-circonato dicálcico por sinterización reactiva de mezclas dolomita – circón; Estudio del procesamiento, Boletín de la Sociedad Española de Cerámica y Vídrio 40 (2001) 463–471.
[15] J.L. Rodríguez, M.A. Rodríguez, S. De Aza, P. Pena, Reaction sintering of zircon dolomite mixtures, Journal of European Ceramic Society 21 (2001) 343–354.
[16] J.L. Rodríguez, S. De Aza, P. Pena, Effect of agglomerate and grain size on the reaction sintering of zircon–dolomite mixtures, British Ceramic Transactions 100 (2001) 91–181.
[17] J.E. Contreras, G.A. Castillo, E.A. Rodríguez, About the influence of electrofused $FeAl_2O_4$ in a refractory base on MgO–$CaZrO_3$ by sintering on this properties, in: Proceedings of the 8th UNITECR' 03, 2003, p. 72.
[18] Eden.A. Rodríguez, G. Alan-Castillo, Jose.E. Contreras, Tushar.K. Das, Microstructure and properties of spinel- magnesia–zirconia-calcium zirconate refractory mixtures, in: Proceedings of the 10th UNITECR' 07, 2007, p. 612.
[19] J.E. Contreras, G.A. Castillo, E.A. Rodríguez, T.K. Das, A.M. Guzmán, Microstructure and properties of hercynite magnesia –calcium zirconate refractory mixtures, Materials Characterization 54 (2005) 354–359.
[20] J. Szczerba, Chemical corrosion of basic refractories by cement kiln materials, Ceramics International 36 (2010) 1877–1885.
[21] H. Kozuka, Y. Kajita, Y. Tuchiya, T. Honda, S. Ohta, New kind of chrome-free (MgO–CaO–ZrO2) bricks for burning zone of rotary cement kiln, in: Proceedings of the 4th UNITECR' 93, 1993, pp. 1027–1037.
[22] H. Kozuka, Y. Kajita, Y. Tuchiya, T. Honda, S. Ohta, Further improvements of MgO–CaO–ZrO2 refractory bricks, in: Proceedings of the 9th UNITECR' 05, 2005.
[23] J. Liddle, N.H. Brett, Phase Equilibria in the System CaO–MgO–Al_2O_3–ZrO_2, Transactions and Journal of the British Ceramic Society 84 (1984) 128–134.
[24] Slag Atlas, in: VDEh (Ed.), 2nd ed., Verlag Staleisen GmbH, D-Düsseldorf, 1995 (Fig. 3.19).